

Kinetics and Mechanism of Solvent Influence on the Lipase-Catalyzed 1,3-Diolein Synthesis

Zitian Wang, Lingmei Dai, Dehua Liu, Hongjuan Liu,* and Wei Du*



Cite This: *ACS Omega* 2020, 5, 24708–24716

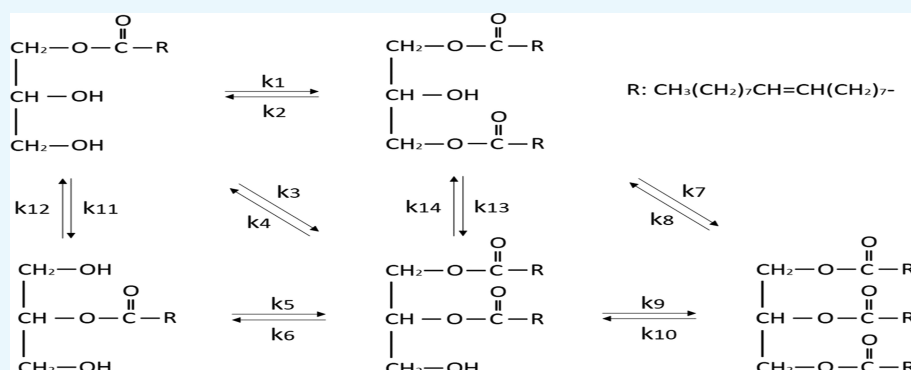


Read Online

ACCESS |

Metrics & More

Article Recommendations



ABSTRACT: 1,3-Diacylglycerol preparation has roused increasing attention in recent years as the 1,3-diacylglycerol-rich oils can suppress the deposition of visceral fat and prevent the body weight increasing. Lipozyme TL IM-mediated esterification of oleic acid with monoolein was effective for 1,3-diacylglycerol production. During the esterification process, the solvent shows obvious influence on the diolein synthesis as well as the 1,3-diolein production. This work investigated the related kinetics and mechanism of the solvent effect on the esterification and Lipozyme TL IM performance. The results indicated that both the esterification rate constant and the acyl migration rate constant positively correlated with the $\log P$ of the solvent, while the site specificity of lipase has negative correlation with solvent $\log P$. The acylation toward the 2-position of 1-monoolein was more sensitive to the solvent $\log P$ compared to the 1-position of glycerides. Molecular dynamics simulation revealed that solvents with different $\log P$ influenced the structure of Lipozyme TL IM including RMSD, hydrogen bond, and radial distribution function to a large extent, which subsequently led to the catalytic activity and selectivity variation of the lipase.

1. INTRODUCTION

Diacylglycerol (DAG) is regarded as the world ahead anti-obesity functional cooking oil and appears in three stereoisomers as sn-1,2-DAG, sn-1,3-DAG, and sn-2,3-DAG.^{1,2} 1,3-DAG was identified of having function on suppressing the accumulation of visceral fat and lowering glucose, cholesterol, and postprandial serum triacylglycerol levels and then preventing the body weight increasing.^{3,4} Herein, as a small natural constituent contained in edible oils and fats, the production of 1,3-DAG has attracted increasing attention.^{5–7} Generally speaking, 1,3-DAG can be produced through enzymatic and chemical methods from oils and fats of plants and animals sources.^{8–11} Although the chemical way is less costly, the process should be performed at very high temperatures (220–260 °C) and result in the heat labile polyunsaturated fatty acid degradation.^{12,13} The enzymatic way is more preferable as it has the superiorities of being environmentally friendly, having mild reaction condition, and being specific in their reaction. The lipases that are used for 1,3-DAG production include lipases from *Thermomyces*

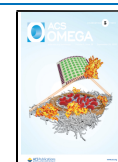
lanuginose, *Mucor javanicus*, *Rhizomucor miehei*, and *Candida Antarctica*.^{14–16} It was reported that the immobilized *Rhizopus oryzae* lipase could keep about 80% of its activity after 60 times of recycling in the esterification of 1,3-DAG production with oleic acid.¹⁶

For the synthesis of 1,3-DAG with lipase as the catalyst, the organic solvents have obvious influence on the enzymatic process, and especially, the $\log P$ of solvents affect the enzyme activity and selectivity greatly.^{17–19} Li et al. studied the effect of organic solvents on the activity and sn-1,3 selectivity of whole-cell lipase from *Aspergillus niger* GZUF36; the lipase showed higher activity in hydrophobic solvents than that in

Received: July 8, 2020

Accepted: September 2, 2020

Published: September 15, 2020



hydrophilic solvents, and the lipase may appear excellent sn-1,3 selectivity only in proper hydrophobic solvents.²⁰

In our previous study, Lipozyme TL IM-mediated esterification of oleic acid with monoolein and glycerol was explored for diolein preparation.^{21,22} With the solvent log*P* increasing, the positional selectivity and diolein yield of the enzyme increased to a maximum and then decreased. It seemed that in the process of multiple reactions involved, reactions are apt to generate the products with log*P* closer to the system log*P*. However, the related mechanism is not very clear. So, it is necessary to investigate the kinetic mechanism of the solvents effect on the lipase structure and function in the esterification process.

As suggested in Figure 1, lipase-mediated 1,3-diolein preparation is quite complicated with several steps involved,

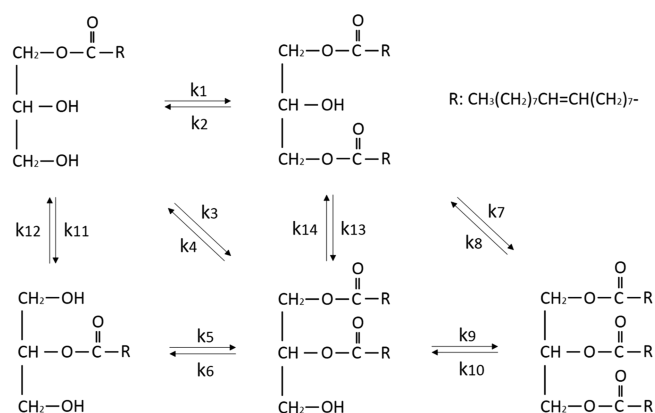


Figure 1. Lipase-mediated esterification of oleic acid with monoolein.

and the acyl migration also occurs in the process. From the kinetic point of view, the ratio of k_1/k_3 can be used to describe

the 1,3-positional selectivity of Lipozyme TL IM to obtain the better understanding of the complicated solvent influence. In addition, molecular dynamics (MD) simulation also is regarded as playing an important role in the study of the relationship between bio-macromolecule's structures and its function, which indicates the atomistic movement of the system based on interatomic potentials, force fields, and Newtonian mechanics.^{23–25} It not only can obtain the micromotion process of lipase in the atomic level but also can learn the information of lipase conformation changes.

In this work, lipase Lipozyme TL IM was used as the catalyst in the esterification of oleic acid with monoolein by using several solvents with different log*P* values. The kinetic solvent effect on the esterification was studied and the kinetic rate constants were calculated. The molecular dynamics simulation was further adopted to discuss the mechanism of the solvent influence on the lipase structure and function in the esterification process of 1,3-diolein preparation. This work enhanced the understanding of the catalyzing mechanism of lipase in different solvent systems, also helpful for the application of lipase in 1,3-DAG synthesis.

2. MATERIALS AND METHODS

2.1. Materials. Lipozyme TL IM (immobilized lipase from *Thermomyces lanuginose*) was obtained from Novozymes (Denmark). Glycerol of pharmaceutical grade (min. 99.7% purity) was purchased from Vance Bioenergy (Malaysia). Oleic acid, 1,2-diolein, 2-monoolein, 1-monoolein, 1,3-diolein, and triolein of chromatographic purity were purchased from Sigma-Aldrich (St. Louis, MO). All other analytical grade reagents were purchased commercially.

2.2. The Original Water Activity Control. Original water activity was controlled by the method of saturated salt solution.²⁶ Before esterification, the lipase, solvents, and

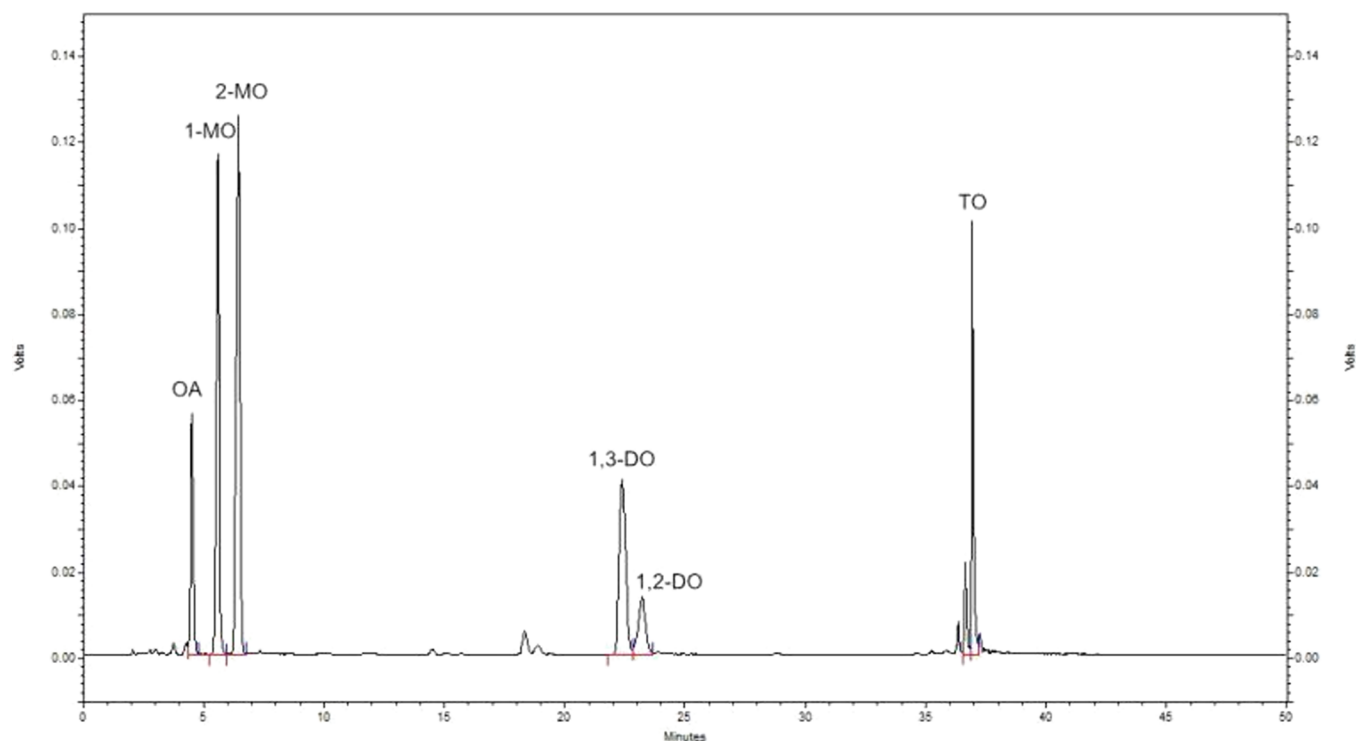


Figure 2. HPLC analysis of the esterification sample.

substrates were equilibrated separately with MgCl_2 saturated salt solution of known a_w (0.33) for 72 h in airtight desiccators.

2.3. 1,3-Diolein Synthesis Procedure. The lipase-mediated catalysis was conducted in a 50 mL shake flask on a rotary shaker at 45 °C and 200 rpm. 1,3-Diolein synthesis was carried out as follows: lipase dosage of 15% (based on oleic acid weight), molar ratio of oleic acid to monoolein of 1.5, solvent weight of 80% (based on oleic acid weight), and water activity of 0.33. Samples of 50 μL were obtained from the reaction mixture. Then, the samples were centrifuged and the upper layer was obtained for HPLC analysis.

2.4. Analysis of the Samples. The content of oleic acid and diacylglycerols in the esterification system were analyzed by a Shimadzu 20A (Shimadzu, Kyoto, Japan) HPLC system with a chromatographic column of C18 column (5 μm , 250 mm \times 4.6 mm) (Dikma Technology, PLATISIL ODS, China) and an ELSD-LT II low-temperature evaporative light scattering detector. The temperature of the column was 40 °C, and the mobile phases were the acetonitrile with 0.15% acetic acid and dichloromethane in a gradient elution program as the reference.²² A total of 1 mL of acetone and 5 μL of the sample were mixed, and then 20 μL of the mixture was used for HPLC analysis. The standard HPLC analysis is shown in Figure 2.

External standards of 1-monoolein, 2-monoolein, 1,2-diolein, 1,3-diolein, triolein, and oleic acid were used to prepare calibration solutions at seven different concentrations. The diolein yield was defined as the molar percentage of the synthesized diolein in the diolein that all the initial glycerol was assumed to be transformed into. The diolein (DO) yield and 1,3-DAG/diolein were calculated as follows:

$$\text{yield}_{\text{DO}} = \frac{m_{\text{DO}}}{m_{\text{glycerol, initial}}} \times 92.09$$

$$1,3\text{-DO}/\text{DO} = \frac{m_{1,3\text{-DO}}}{m_{\text{total-DO}}}$$

2.5. Calculation of Reaction Rate Constants. The enzymatic reaction mechanism was briefly described in Figure 1. During the reaction, the esterification reaction rate would follow the second-order reversible reaction kinetics to the concentration of each substrate,²⁷ and the acyl migration process followed the first-order reversible reaction. The mass transfer limitation could be neglected in the esterification system. According to the above assumptions, the differential equations describing the reaction were set up and shown in Figure 3.

In the equations, [1-MO], [2-MO], [OA], [1,3-DO], [1,2-DO], and [TO] referred to the concentration of 1-monoolein, 2-monoolein, oleic acid, 1,3-diolein, 1,2-diolein, and triolein, respectively. The reaction rate constant was calculated by the software Matlab.

2.6. Molecular Dynamics Simulation. The molecular dynamics simulation was performed with the software GROMACS 4.0.1. The structure of the lipase Lipozyme TL IM was acquired from the Brookhaven Protein Data Bank, and the PDB code is 1DTE. The lipase was put into the center of a dodecahedron box with a side length of 3.0 nm. There was one lipase molecule and a certain number of solvent molecules in the system. The leap-frog algorithm was used to integrate the

$$\begin{aligned} \frac{d[\text{OA}]}{dt} &= k_2[1,3\text{-DO}] + (k_4 + k_6)[1,2\text{-DO}] + (k_8 + k_{10})[\text{TO}] \\ &\quad - (k_1 + k_3)[1\text{-MO}][\text{OA}] - k_7[1,3\text{-DO}][\text{OA}] \\ &\quad - k_5[2\text{-MO}][\text{OA}] - k_9[1,2\text{-DO}][\text{OA}] \\ \frac{d[1\text{-MO}]}{dt} &= k_2[1,3\text{-DO}] + k_{12}[2\text{-MO}] + k_{11}[1,2\text{-DO}] - k_1[1\text{-MO}][\text{OA}] \\ &\quad - k_{11}[1\text{-MO}] - k_3[1\text{-MO}][\text{OA}] \\ \frac{d[2\text{-MO}]}{dt} &= k_{11}[1\text{-MO}] + k_6[1,2\text{-DO}] - k_{12}[2\text{-MO}] - k_5[2\text{-MO}][\text{OA}] \\ \frac{d[1,3\text{-DO}]}{dt} &= k_{11}[1\text{-MO}][\text{OA}] + k_{14}[1,2\text{-DO}] + k_3[\text{TO}] \\ &\quad - k_2[1,3\text{-DO}] - k_{13}[1,3\text{-DO}] - k_7[1,3\text{-DO}][\text{OA}] \\ \frac{d[1,2\text{-DO}]}{dt} &= k_3[1\text{-MO}][\text{OA}] + k_{13}[1,3\text{-DO}] + k_5[2\text{-MO}][\text{OA}] + k_{10}[\text{TO}] \\ &\quad - k_4[1,2\text{-DO}] - k_6[1,2\text{-DO}] - k_{14}[1,2\text{-DO}] - k_9[1,2\text{-DO}][\text{OA}] \\ \frac{d[\text{TO}]}{dt} &= k_7[1,3\text{-DO}][\text{OA}] + k_9[1,2\text{-DO}][\text{OA}] - k_8[\text{TO}] - k_{10}[\text{TO}] \end{aligned}$$

Figure 3. Differential equations of the esterification of oleic acid with monoolein.

Newtonian equations and the time step was 0.002 ps. The LINC algorithm was used for the bond constraint.

Before the simulation, the system was submitted to 500 steps of steepest descent minimization to converge the system's energy to 2000 $\text{kJ}\cdot\text{mol}^{-1}\cdot\text{nm}^{-1}$. For keeping the protein coordinate fixed and equilibrating the solvent simulation, a 10 ps position-restrained molecular dynamics simulation was adopted for 1000 ps at 318 K.

The parameters including root mean square distance (RMSD), hydrogen bond (H-bond) number, and radial distribution function (RDF) were obtained from the simulation to evaluate the effect of solvents on the lipase structure and function in the esterification process.

3. RESULTS AND DISCUSSION

3.1. Kinetics in the Enzymatic Esterification of 1,3-Diolein Preparation. Organic solvent plays a significant role in the non-aqueous phase enzymatic process. It was reported that $\log P$ of solvents correlated with the enzyme activity and selectivity obviously.^{18,19} So, the kinetics of the solvents with different $\log P$ values was studied in the esterification process of 1,3-diolein preparation. Because the water activity of the reaction system influences the enzyme activity,^{20,22,28} all the reactions were controlled at the same water activity. Five solvents containing *t*-butanol, *t*-amyl alcohol, toluene, hexamethylene, and *n*-hexane with different $\log P$ values of 0.80, 1.15, 2.5, 3.2, and 3.5 at the same water activity 0.33 were used in the experiment to assess the effect of solvent $\log P$ on the esterification of 1,3-diolein preparation. The esterification rate constant (k_1 – k_{10}), acyl migration rate constant (k_{11} – k_{14}), and 1,3-positional selectivity (k_1/k_3) rate constant were calculated and shown in Table 1.

As indicated in Table 1, the rate constant was different with the different solvents. The correlation between the solvent $\log P$ and the esterification rate constant is shown in Figure 44a–d. With the increasing of solvent $\log P$, the esterification rate constant (k_1 – k_{10}) enhanced, and the acyl migration rate constant (k_{11} – k_{14}) also increased at the same time. It is may be because that lipase can maintain higher catalytic activity in relatively hydrophobic solvents (high $\log P$). In addition, the acyl migration rate also could be affected by the solvent polarity through its influence on the charge dispersion of the transition state.²⁹ The solvent with low polarity (high $\log P$) was favorable for the transition state charge dispersion and its

Table 1. Rate constant^a of the Enzymatic Esterification for 1,3-Diolein Preparation

solvent	<i>t</i> -butanol	<i>t</i> -amyl alcohol	toluene	hexamethylene	<i>n</i> -hexane
log <i>P</i>	0.80	1.15	2.50	3.20	3.50
<i>k</i> ₁	0.1212	0.1636	0.3955	0.4854	0.5190
<i>k</i> ₂	0.0500	0.0700	0.0797	0.0831	0.0880
<i>k</i> ₃	0.0006	0.0015	0.0066	0.0097	0.0160
<i>k</i> ₄	0.0013	0.0049	0.0068	0.0074	0.0147
<i>k</i> ₅	0.2531	0.3286	0.8032	0.9001	1.1610
<i>k</i> ₆	0.0215	0.0380	0.0400	0.0411	0.0470
<i>k</i> ₇	0.0006	0.0012	0.0037	0.0050	0.0152
<i>k</i> ₈	0.0008	0.0010	0.0018	0.0024	0.0032
<i>k</i> ₉	0.0800	0.1003	0.2310	0.2503	0.4515
<i>k</i> ₁₀	0.0070	0.0080	0.0085	0.0090	0.0100
<i>k</i> ₁₁	0.0133	0.0146	0.0290	0.0800	0.2012
<i>k</i> ₁₂	0.0644	0.0797	0.4010	0.9580	1.1405
<i>k</i> ₁₃	0.0206	0.0283	0.1010	0.2490	0.4068
<i>k</i> ₁₄	0.0408	0.0500	0.1857	0.5320	1.0207
<i>k</i> ₁ / <i>k</i> ₃	202.0000	109.0667	59.9242	50.0412	32.4375

^aUnit of rate constant: *k*₁–*k*₁₀ (L·mol⁻¹·h⁻¹), *k*₁₁–*k*₁₄ (h⁻¹).

energy state would be lower, which resulted in the increase of the acyl migration rate.

Lipase TL IM has been demonstrated as a 1,3-specific enzyme, and the kinetics study also confirmed that. The value of *k*₁/*k*₃ declined with the increasing of solvent log*P* (Table 1, Figure 4d). It may indicate that comparing with the 1-position of the 1-monoolein molecular, the acylation of 2-position was more sensitive to the solvent log*P* and the related mechanism need to be explored further.

3.2. Molecular Dynamics Simulation of Lipozyme TL IM in Esterification of 1,3-Diolein Preparation with Different Solvents. The above results suggested that organic solvents with different log*P* values had obvious influence on the Lipozyme TL IM-catalyzed esterification. Molecular dynamics simulation was further adopted to explore the mechanism of solvent influence on the lipase structure and function in the esterification process, and the values of RMSD (root-mean-square deviation), H-bond, and RDF (radial distribution function) were analyzed.

3.2.1. Solvents Influence on RMSD. The RMSD value can reflect the specific conformation difference of the enzyme. Relatively lower RMSD value suggests high stability of the enzyme conformation, while the relatively higher value of RMSD indicates that the conformation of the enzyme changes a lot and is not stable.^{30,31} In our simulation, the original enzyme conformation was inactive, so the higher value of RMSD might mean a higher possibility of the enzyme conformation changing to be active and subsequently leading to higher activity.

The simulation was carried out with the lipase Lipozyme TL IM in six different solvent esterification systems including toluene, hexamethylene, *n*-hexane, acetone, *t*-butanol, and *t*-amyl alcohol. The dynamic RMSD value of the lipase active site, the lipase lid, and the whole lipase molecule was calculated, respectively. (Figure 5, Figure 5b, Figure 5c). The RMSD value of the enzyme active site changed little for all the six solvents, indicating that the active site conformation of lipase Lipozyme TL IM was stable with the tested six organic solvents. The RMSD value of the lid changed little for the relatively hydrophobic solvents (i.e., toluene, hexamethylene,

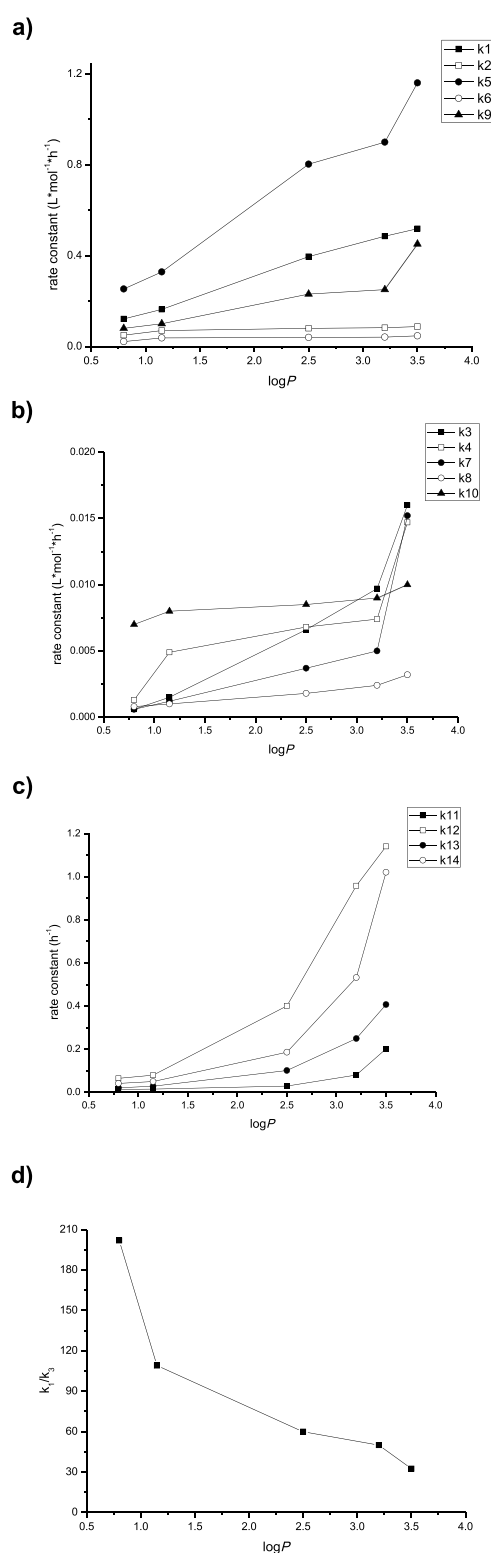


Figure 4. (a) Correlation between solvent log*P* and esterification rate constants *k*₁, *k*₂, *k*₅, *k*₆, and *k*₉. (b) Correlation between solvent log*P* and esterification rate constants *k*₃, *k*₄, *k*₇, *k*₈, and *k*₁₀. (c) Correlation between solvent log*P* and acyl migration rate constants *k*₁₁–*k*₁₄. (d) Correlation between solvent log*P* and 1,3-positional selectivity (*k*₁/*k*₃) of Lipozyme TL IM.

n-hexane), but it varied obviously for the relatively hydrophilic solvents (i.e., acetone, *t*-butanol, and *t*-amyl alcohol) (Figure 5b). Therefore, the stability of the lipase lid in hydrophobic

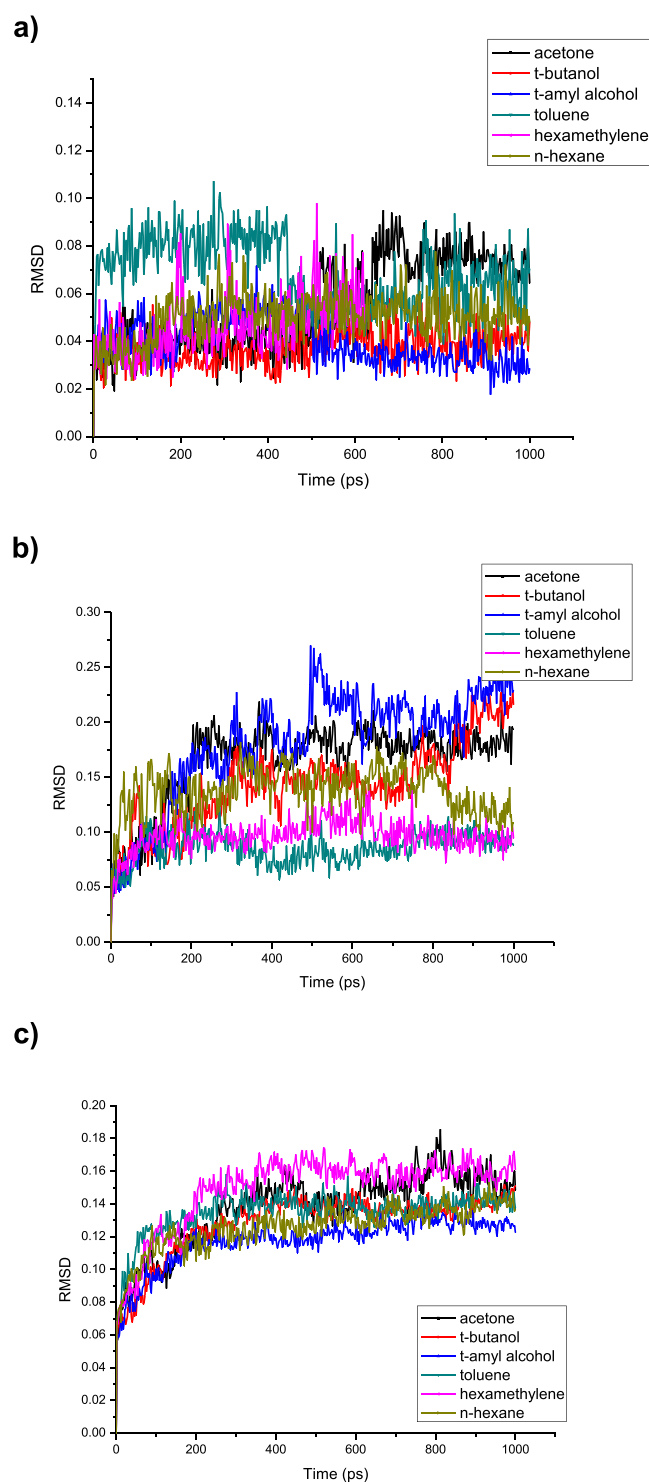


Figure 5. (a) Solvent influence on the RMSD value of the lipase's active site. (b) Solvent influence on the RMSD value of the lipase's lid. (c) Solvent influence on the RMSD value of the whole lipase molecule.

solvents was much higher than that in the hydrophilic solvents. The RMSD value of the whole lipase molecule also was calculated and it was quite stable in the simulation of 300 ps for all the six solvents (Figure 5c).

The difference of the average RMSD value in different solvents could reflect the variation of the lipase structure and function.^{30,31} The average RMSD value of the lipase active site,

lipase lid, and whole lipase molecule were also calculated and shown in Figure 6a–c.

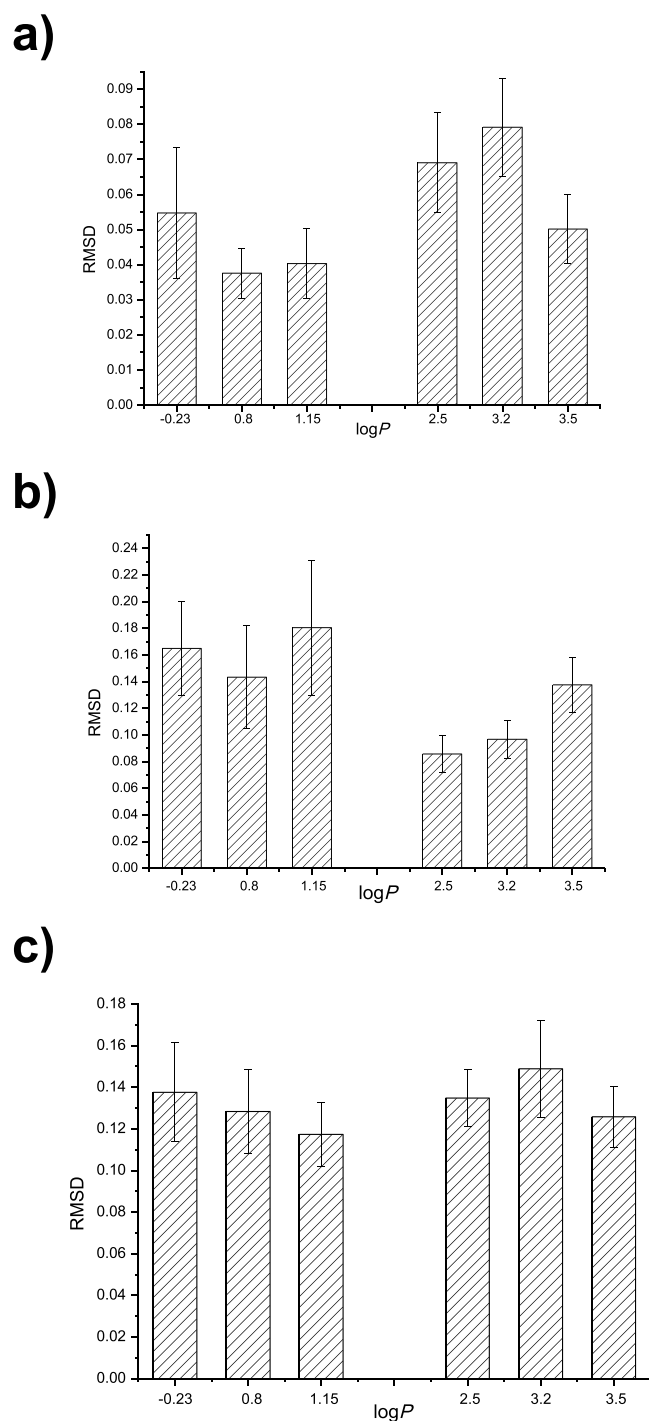


Figure 6. (a) Solvent influence on the average RMSD value of the lipase's active site. (b) Solvent influence on the average RMSD value of the lipase's lid. (c) Solvent influence on the average RMSD value of the whole lipase molecule.

The average RMSD value of the active site was higher for the relatively hydrophobic solvents ($\log P > 2$) than that of the hydrophilic solvent ($\log P < 2$). It indicated that the conformation of lipase active site had higher possibility to be activated in the relatively hydrophobic solvents, which resulted in a higher activity of the lipase. Moreover, the average RMSD

value of the lid was higher in the relatively hydrophilic solvents ($\log P < 2$) than that of the hydrophobic solvent ($\log P > 2$). It suggested that the conformation of lipase lid had higher possibility to be activated in the relatively hydrophilic solvents, which led to a higher selectivity of the lipase. In addition, the average RMSD value of the whole lipase molecule had no obvious correlation with the solvent $\log P$. The simulation results were in accordance with the experiment phenomena. With the enhancement of solvent $\log P$, the lipase catalytic activity increased and 1,3-positional selectivity decreased. Li et al. studied the organic solvent effect on the sn-1,3 selectivity and activity of whole-cell lipase from *Aspergillus niger* GZUF36. Solvent polarity influenced the sn-1,3 selectivity of the whole-cell lipase obviously. The higher the polarity, the lower the sn-1,3 selectivity was observed. However, for the enzymatic activity, lipase showed higher activity in hydrophobic solvent than that in the hydrophilic one.²⁰

3.2.2. Solvent Influence on H-Bond. The value of H-bond reflects the rigidity of enzyme. The higher value of the enzyme H-bond indicates higher rigidity and lower flexibility of enzyme, while the lower H-bond value means lower rigidity and higher flexibility of the enzyme. Simulation with the lipase Lipozyme TL IM in six different solvent esterification systems were carried out, and the H-bond values were compared and shown in Figure 7a–c.

As Figure 7a shown, the H-bond value of the lipase active site was lower in relatively hydrophobic solvents than that in the hydrophilic solvent system. So, the active site flexibility of the lipase Lipozyme TL IM in the hydrophobic solvent system was higher and the lipase active site was much easier to form a transition state with the substrate, which led to the higher catalytic activity of lipase in the hydrophobic solvent system. The H-bond value of the lid was lower in the relatively hydrophilic solvent (Figure 7b). The possible reason was that the higher flexibility of the lid in the hydrophilic solvent prevented the substrate from entering into the cracks and holes to interact with the lipase active site. For the whole lipase molecule, the H-bond value was higher in the relatively hydrophobic solvent system (Figure 7c), which might be due to the charged amino acid chain of the lipase folded to the surface and formed more hydrogen bonds to stabilize the protein structure. Hydrogen bonds and their relative strength in a water environment are necessary to enhance the protein–ligand binding.³² According to the study of Gao et al., a hydrogen bond forms when an electronegative atom in a H-bond acceptor nears to a hydrogen atom bonded to another electronegative atom in a H-bond donor.³³ The results obtained could be used to explain the phenomenon in the above sections where the lipase's catalytic activity was higher in the solvents with high $\log P$.

3.2.3. Solvents Influence on RDF. The value of RDF (radial distribution function, $g(r)$) can reflect the distribution of solvent molecules around the lipase. The higher RDF value means that there are more solvent molecules in the specific area around the lipase. Simulation with the lipase Lipozyme TL IM in six different solvent esterification systems were carried out, and the results are indicated and shown in Figure 8a,b.

As Figure 8a,b suggested, the solvent molecules could interact with the lipase active site and lid to form a hydrogen bond when the distance between them was within 0.35 nm, and the solvent molecules near the lipase might strip water from the lipase surface. Then, the minimum distance from the lipase lid and active site to the different solvent molecules was

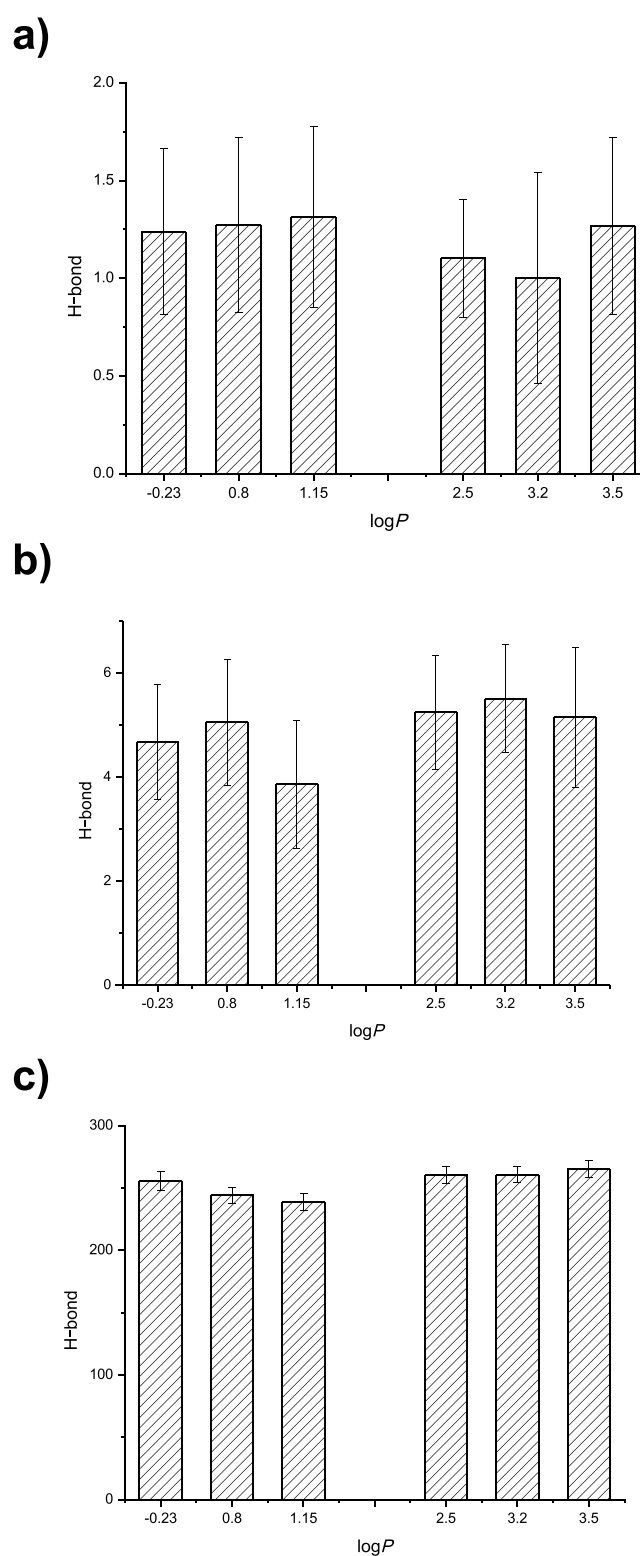


Figure 7. (a) Solvent influence on the H-bond value of the lipase active site. (b) Solvent influence on the H-bond value of the lipase lid. (c) Solvent influence on the H-bond value of the whole lipase molecule.

calculated and the probability density of the solvent molecules in the 0.35 nm radial distance area of lipase was investigated. The results are shown in Figure 9a–d.

The results indicated that the solvent molecules were closer to the active site and lid in the relatively hydrophilic solvents

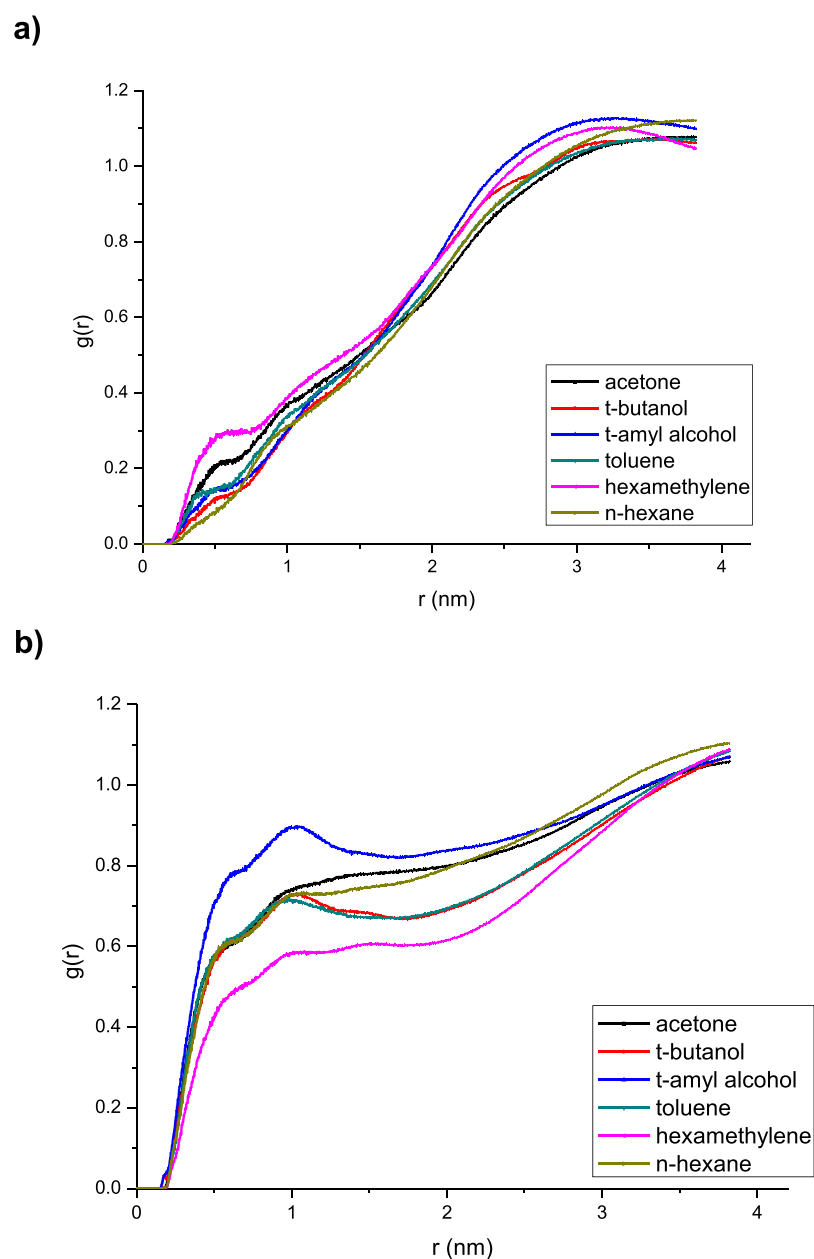


Figure 8. Solvent influence on the RDF value of the lipase active site. (b) Solvent influence on the RDF value of the lipase lid.

than that of hydrophobic solvents, which might make it easier for the solvent molecule to strip the water from the lipase surface, and then lead to the decrease of lipase activity (Figure 9a,b). There was no obvious correlation between the solvent $\log P$ and the probability density of solvent molecules in the 0.35 nm radial distance area around the lipase active site (Figure 9c). However, the probability density of solvent molecules in the 0.35 nm radial distance area around the lid was higher for the relatively hydrophobic solvents than that of hydrophilic solvents (Figure 9d). It suggested that the relatively hydrophilic solvent molecules were much easier to interact with the lipase's lid (Figure 9d). Chen et al.³⁴ studied the conformational stability of porcine pancreatic lipase in the solvents of dimethyl sulfoxide, propylene glycol, and ethanol with molecular dynamics simulation. The active pocket RMSD in all solvents enhanced with the solvent $\log P$ increasing, while the R_g and H-bond between the solvent and lipase decreased, indicating that lipase in dimethyl sulfoxide exhibited the

highest enzyme–substrate affinity.³⁴ So, molecular dynamics simulation is very useful in exploring the protein structure and understanding the characteristics of the enzymes at the atomic and molecular level.

4. CONCLUSIONS

Lipase-catalyzed reaction of oleic acid with monoolein was promising for the production of 1,3-diolein. The effect of solvents on the catalytic performance of 1,3-diolein production was investigated from the kinetic point of view. The solvents with different $\log P$ values showed obvious influence on the diolein synthesis as well as the 1,3-diacylglycerol production. During the esterification process with lipase Lipozyme TL IM as the catalyst, the rate constant including the esterification rate constant and acyl migration rate constant increased with the enhancement of the solvent $\log P$, while the lipase 1,3-positional selectivity decreased. The molecular dynamics

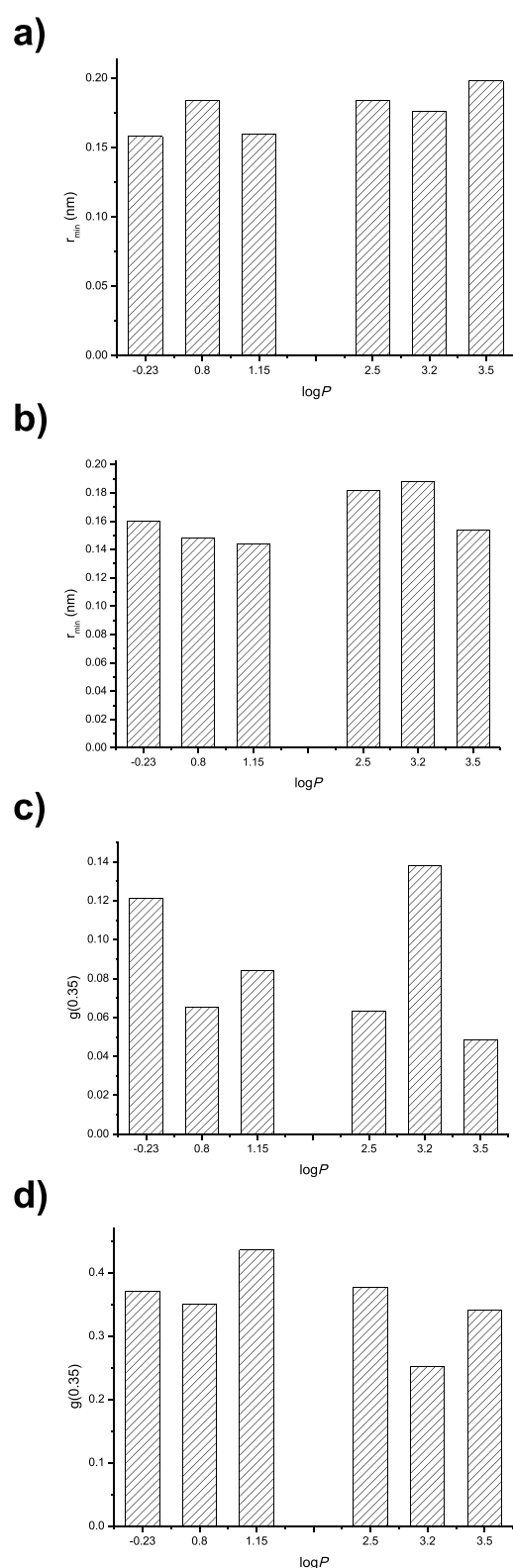


Figure 9. (a) Minimum distance of solvent from the lipase active site. (b) Minimum distance of solvent from the lipase lid. (c) Probability density of solvent in the 0.35 nm radial distance area around the active site of lipase. (d) Probability density of solvent in the 0.35 nm radial distance area around the lid of lipase.

simulation was further investigated, and the results revealed that solvents with different $\log P$ values could affect the lipase's structure, including the RMSD, H-bond, and RDF, which

correspondingly influenced the lipase catalytic activity and selectivity.

AUTHOR INFORMATION

Corresponding Authors

Hongjuan Liu – Institute of Nuclear and New Energy Technology, Tsinghua University, Beijing 100084, P.R. China; orcid.org/0000-0001-8815-9355; Email: liuhongjuan@tsinghua.edu.cn

Wei Du – Key Laboratory for Industrial Biocatalysis, Ministry of Education, Department of Chemical Engineering, Tsinghua University, Beijing 100084, China; Tsinghua Innovation Center in Dongguan, Dongguan, Guangdong 523808, P.R. China; orcid.org/0000-0003-4094-210X; Phone: +86-10-62772130; Email: duwei@tsinghua.edu.cn; Fax: +86-10-62785475

Authors

Zitian Wang – Key Laboratory for Industrial Biocatalysis, Ministry of Education, Department of Chemical Engineering, Tsinghua University, Beijing 100084, China

Lingmei Dai – Key Laboratory for Industrial Biocatalysis, Ministry of Education, Department of Chemical Engineering, Tsinghua University, Beijing 100084, China

Dehua Liu – Key Laboratory for Industrial Biocatalysis, Ministry of Education, Department of Chemical Engineering, Tsinghua University, Beijing 100084, China; Tsinghua Innovation Center in Dongguan, Dongguan, Guangdong 523808, P.R. China

Complete contact information is available at: <https://pubs.acs.org/10.1021/acsomega.0c03284>

Notes

The authors declare no competing financial interest.

ACKNOWLEDGMENTS

The authors express their gratitude to the support from the Dongguan Science & Technology Bureau (Innovative R&D Team Leadership of Dongguan City, 201536000100033), the National Nature Science Foundation of China (no. 21676159), and the China-Latin America Joint Laboratory for Clean Energy and Climate Change (KY201501004).

REFERENCES

- Lee, W. J.; Zhang, Z.; Lai, O. M.; Tan, C. P.; Wang, Y. Diacylglycerol in food industry: Synthesis methods, functionalities, health benefits, potential risks and drawbacks. *Trends Food Sci. Technol.* **2020**, *97*, 114–125.
- Lee, Y.-Y.; Tang, T.-K.; Phuah, E.-T.; Tan, C.-P.; Wang, Y.; Li, Y.; Cheong, L.-Z.; Lai, O.-M. Production, safety, health effects and applications of diacylglycerol functional oil in food systems: A review. *Crit. Rev. Food. Sci. Nutr.* **2020**, *60*, 2509–2525.
- Lee, A.; Yoo, H. J.; Kim, M.; Kim, M.; Choi, J.-H.; Lee, C.; Lee, J. H. Effects of equivalent medium-chain diacylglycerol or long-chain triacylglycerol oil intake via muffins on postprandial triglycerides and plasma fatty acids levels. *J. Funct. Foods* **2019**, *53*, 299–305.
- Morita, O.; Soni, M. G. Safety assessment of diacylglycerol oil as an edible oil: a review of the published literature. *Food Chem. Toxicol.* **2009**, *47*, 9–21.
- Zhao, J.-f.; Lin, J.-p.; Yang, L.-r.; Wu, M.-b. Enhanced performance of *Rhizopusoryzae* lipase by reasonable immobilization on magnetic nanoparticles and its application in synthesis 1,3-diacylglycerol. *Appl. Biochem. Biotechnol.* **2019**, *188*, 677–689.
- Guo, Y.; Cai, Z.; Xie, Y.; Ma, A.; Zhang, H.; Rao, P.; Wang, Q. Synthesis, physicochemical properties, and health aspects of

structured lipids: A review. *Compr. Rev. Food Sci. Food Saf.* **2020**, *19*, 759–800.

(7) Dosso, L. A.; Luggren, P. J.; Di Cosimo, J. I. Synthesis of Edible Vegetable Oils Enriched with Healthy 1,3-Diglycerides Using Crude Glycerol and Homogeneous/Heterogeneous Catalysis. *J. Am. Oil Chem. Soc.* **2020**, *97*, 551–561.

(8) Palacios, D.; Ortega, N.; Rubio-Rodríguez, N.; Busto, M. D. Lipase-catalyzed glycerolysis of anchovy oil in a solvent-free system: Simultaneous optimization of monoacylglycerol synthesis and end-product oxidative stability. *Food Chem.* **2019**, *271*, 372–379.

(9) Diao, X.; Guan, H.; Kong, B.; Zhao, X. Preparation of diacylglycerol from lard by enzymatic glycerolysis and its compositional characteristics. *Korean J. Food. Sci. Anim. Resour.* **2017**, *37*, 813–822.

(10) Zhong, N.; Chen, W.; Liu, L.; Chen, H. Immobilization of *Rhizomucor miehei* lipase onto the organic functionalized SBA-15: Their enzymatic properties and glycerolysis efficiencies for diacylglycerols production. *Food Chem.* **2019**, *271*, 739–746.

(11) Zhong, N.; Li, Y.; Cai, C.; Gao, Y.; Liu, N.; Liu, G.; Tan, W.; Zheng, Y. Enhancing the catalytic performance of *Candida Antarctica* lipase B by immobilization onto the ionic liquids modified SBA-15. *Eur. J. Lipid Sci. Technol.* **2018**, *120*, 1700357.

(12) Satriana; Arpi, N.; Lubis, Y. M.; Adisalamun; Supardan, M. D.; Mustapha, W. A. W. Diacylglycerol-enriched oil production using chemical glycerolysis. *Eur. J. Lipid Sci. Technol.* **2016**, *118*, 1880–1890.

(13) Subroto, E.; Wisamputri, M. F.; Supriyanto; Utami, T.; Hidayat, C. Enzymatic and chemical synthesis of high mono- and diacylglycerol from palm stearin and olein blend at different type of reactor stirrers. *J. Saudi Soc. Agric. Sci.* **2020**, *19*, 31–36.

(14) Laguerre, M.; Mputu, M. N.; Briys, B.; Lopez, M.; Villeneuve, P.; Dubreucq, E. Regioselectivity and fatty acid specificity of crude lipase extracts from *Pseudozyma tsukubaensis*, *Geotrichum candidum*, and *Candida rugosa*. *Eur. J. Lipid Sci. Technol.* **2017**, *119*, 1600302.

(15) Liu, N.; Li, D.; Wang, W.; Hollmann, F.; Xu, L.; Ma, Y.; Yang, B.; Bai, W.; Sun, X.; Wang, Y. Production and immobilization of lipase PCL and its application in synthesis of α -linolenic acid-rich diacylglycerol. *J. Food Biochem.* **2018**, *42*, No. e12574.

(16) Zhao, J.-f.; Tao-Wang; Lin, J.-p.; Yang, L.-r.; Wu, M.-B. Preparation of high-purity 1,3-diacylglycerol using performance-enhanced lipase immobilized on nanosized magnetite particles. *Biotechnol. Bioprocess Eng.* **2019**, *24*, 326–336.

(17) Yang, T.; Zhang, H.; Mu, H.; Sinclair, A. J.; Xu, X. Diacylglycerols from butterfat: production by glycerolysis and short-path distillation and analysis of physical properties. *J. Am. Oil Chem. Soc.* **2004**, *81*, 979–987.

(18) Carrea, G.; Ottolina, G.; Riva, S. Role of solvents in the control of enzyme selectivity in organic media. *Trends Biotechnol.* **1995**, *13*, 63–70.

(19) Giacometti, J.; Giacometti, F. Study of organic solvent hydrophobicity on lipase catalyzed reaction esterification. *Chem. Biochem. Eng. Q.* **2006**, *20*, 260–274.

(20) Li, C.; Zhang, F.; Gao, Z.; He, L.; Zeng, X.; Zhu, Q.; Yu, L. Effects of organic solvent, water activity, and salt hydrate pair on the sn-1,3 selectivity and activity of whole-cell lipase from *Aspergillus niger* GZUF36. *Appl. Microbiol. Biotechnol.* **2018**, *102*, 225–235.

(21) Wang, Z.; Su, J.; Du, W.; Liu, D. Lipozyme TL IM-catalyzed Esterification of Oleic Acid for 1,3-Diacylglycerol Preparation. *Chem. J. Chin. Univ.* **2015**, *36*, 1535–1541.

(22) Wang, Z.; Du, W.; Dai, L.; Liu, D. Study on Lipozyme TL IM-catalyzed Esterification of Oleic acid and glycerol for 1,3-diolein Preparation. *J. Mol. Catal. B: Enzym.* **2016**, *127*, 11–17.

(23) Karplus, M.; McCammon, J. A. Molecular dynamics simulations of biomolecules. *Nat. Struct. Biol.* **2002**, *9*, 646–652.

(24) Monhemi, H.; Housaindokht, M. R.; Moosavi-Movahedi, A. A.; Bozorgmehr, M. R. How a protein can remain stable in a solvent with high content of urea: insights from molecular dynamics simulation of *Candida antarctica* lipase B in urea: choline chloride deep eutectic solvent. *J. Chem. Soc., Faraday Trans.* **2014**, *16*, 14882–14893.

(25) Monhemi, H.; Dolatabadi, S. Molecular dynamics simulation of high-pressure CO₂ pasteurization reveals the interfacial denaturation of proteins at CO₂/water interface. *J. CO₂ Util.* **2020**, *35*, 256–264.

(26) Ducret, A.; Trani, M.; Lortie, R. Lipase-catalyzed enantioselective esterification of ibuprofen in organic solvents under controlled water activity. *Enzyme Microb. Technol.* **1998**, *22*, 212–216.

(27) Hazarika, S.; Goswami, P.; Dutta, N. N. Lipase catalyzed transesterification of 2-o-benzylglycerol with vinyl acetate: solvent effect. *Chem. Eng. J.* **2003**, *94*, 1–10.

(28) Halling, P. J. Thermodynamic predictions for biocatalysis in nonconventional media: theory, tests, and recommendations for experimental design and analysis. *Enzyme Microb. Technol.* **1994**, *16*, 178–206.

(29) Mulalee, S.; Srisuwan, P.; Phisalaphong, M. Influences of operating conditions on biocatalytic activity and reusability of Novozym 435 for esterification of free fatty acids with short-chain alcohols: A case study of palm fatty acid distillate. *Chin. J. Chem. Eng.* **2015**, *23*, 1851–1856.

(30) Kumar, C. V.; Swetha, R. G.; Anbarasu, A.; Ramaiah, S. Computational analysis reveals the association of threonine 118 methionine mutation in Pmp22 resulting in CMT-1A. *Adv. Bioinf.* **2014**, *2014*, 502618.

(31) Pandey, B.; Grover, A.; Sharma, P. Molecular dynamics simulations revealed structural differences among WRKY domain-DNA interaction in barley (*Hordeum vulgare*). *BMC Genomics* **2018**, *19*, 132.

(32) Chen, D.; Oezguen, N.; Urvil, P.; Ferguson, C.; Dann, S. M.; Savidge, T. C. Regulation of protein-ligand binding affinity by hydrogen bond pairing. *Sci. Adv.* **2016**, *2*, No. e1501240.

(33) Gao, Y.; Mei, Y.; Zhang, J. Z. Treatment of hydrogen bonds in protein simulations. In *Advanced materials for renewable hydrogen production, storage and utilization*. Published by IntechOpen: Limited, 2015, p.121.

(34) Chen, Z.-S.; Wu, Y.-D.; Hao, J.-H.; Liu, Y.-J.; He, K.-P.; Jiang, W.-H.; Xiong, M.-J.; Lv, Y.-S.; Cao, S.-L.; Zhu, J. Molecular Dynamic Simulation of the Porcine Pancreatic Lipase in Non-aqueous Organic Solvents. *Front. Bioeng. Biotechnol.* **2020**, *8*, 676.